

Heat capacity from local moments in frustrated disordered quantum spin systems: scaling and data collapse

Itamar Kimchi,¹ John P. Scheckton,² Tyrel M. McQueen,^{2,3} and Patrick A. Lee¹

¹*Department of Physics, Massachusetts Institute of Technology, Cambridge, MA 02139, USA*

²*Department of Chemistry, Department of Physics and Astronomy,*

and the Institute for Quantum Matter, The Johns Hopkins University, Baltimore, MD 21218, USA

³*Department of Materials Science and Engineering,*

The Johns Hopkins University, Baltimore, MD 21218, USA

(Dated: February 27, 2018)

Recently measurements on various spin-1/2 quantum magnets such as $H_3\text{LiIr}_2\text{O}_6$, $\text{LiZn}_2\text{Mo}_3\text{O}_8$, $\text{ZnCu}_3(\text{OH})_6\text{Cl}_2$ and 1T-TaS₂ — all described by magnetic frustration and quenched disorder but with no other common relation — nevertheless showed apparently universal scaling features at low temperature. In particular the heat capacity $C[H, T]$ in temperature T and magnetic field H exhibits T/H data collapse reminiscent of scaling near a critical point. Here we propose a theory for this scaling collapse based on an emergent random-singlet regime extended to include spin-orbit coupling and antisymmetric Dzyaloshinskii-Moriya (DM) interactions. We derive the scaling $C[H, T]/T \sim H^{-\gamma} F_q[T/H]$ with $F_q[x] = x^q$ at small x , with $q \in \{0, 1, 2\}$ an integer exponent whose value depends on spatial symmetries. The agreement with experiments indicates that a fraction of spins form random valence bonds and that these are surrounded by a quantum paramagnetic phase. We also discuss distinct scaling for magnetization with a q -dependent subdominant term enforced by Maxwell's relations.

Heat capacity and its temperature and magnetic field dependence is a powerful tool to provide fundamental thermodynamical information on various solids including correlated electrons in magnetic Mott insulators. It has come to our attention that recent measurements of the heat capacity of certain quantum magnets which are candidates for an exotic state of matter called quantum spin liquid¹ show a power law temperature dependence and a striking one-parameter scaling and data collapse as a function of temperature T and magnetic field H . Though the materials all appear quite different the observed scaling functions of $C[H, T]$ as power laws in T/H suggest an unexpected hidden universality.

Power-law specific heat is a familiar consequence of the *random singlet* phase seen in doped semiconductors such as Si:P, and described theoretically in 1D by Dasgupta, Ma and Fisher^{2,3} and in 2D and 3D by Bhatt and Lee^{4–6}. In this picture the spins interact with each other via a broad distribution of antiferromagnetic exchange interactions. The spins that are most strongly coupled pair into singlets first, leaving behind spins that are further apart, eventually resulting in a power law distribution of exchanges and a power law tail of density of states. This picture follows from renormalization group analysis in 1D and has been demonstrated numerically in higher dimensions under a variety of conditions. Though the original setting for the $D > 1$ random-singlet phase required a dilute random network of spin-1/2 sites, without a lattice, recently a random-singlet regime has been argued to arise as a general feature of spin-1/2 lattice magnets with quantum paramagnetic ground states and random exchange energies, i.e. in highly-frustrated quantum magnets with quenched disorder.⁷ The theory applies when the majority of spin-1/2 sites form a paramagnetic state such as a spin liquid or a valence bond

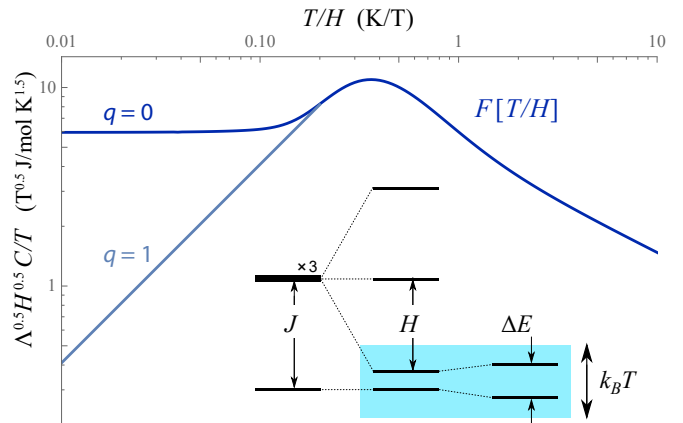


FIG. 1. $C[H, T]$ scaling function $F_0[T/H]$ and its $q=1, 2$ modification by level repulsion. The heat capacity of $q=0$ random singlets (plotted here for integrated energy distribution $\int P[E] = (E/\Lambda)^{1-\gamma}$ at $\gamma = 0.5$, dark blue) exhibits scaling collapse in T/H with T -linear form at $T \ll H$. This is easily understood (bottom inset). A spin-1/2 pair with singlet-triplet splitting J acquires a resonance in magnetic fields $H \approx J$, contributing to heat capacity when $|J - H| < k_B T$. This T -linear scaling is modified when spin-orbit coupling and lattice symmetries combine into DM interactions with singlet-triplet mixing: the resulting level repulsion changes the resonance condition $\Delta E < k_B T$ to produce T -scaling at a higher power, as in the asymptotic $q=1$ line shown (gray).

crystal, and demonstrates in two different controlled limits that a small fraction of sites necessarily nucleates⁸ and leads to a random network of spin-1/2 moments at low energies. This small subsystem may be captured by a random-singlet regime in its low temperature renormalization group flow, developing a power-law proba-

bility distribution of antiferromagnetic exchange energies $P[J] \sim J^{-\gamma}$. At a given temperature T , the spins with exchange $J < T$ behave as free spins giving rise to a heat capacity $C[T] \sim T^{1-\gamma}$ and spin susceptibility $\chi[T] \sim T^{-\gamma}$. In many cases the measurable response from this relatively small emergent subsystem may dominate over the response of the bulk phase. Such an emergent power-law energy distribution, associated with a relatively small portion of the spin-1/2 sites, serves as the *a priori* starting point for the present work.

The power-law distribution of entropy manifests most dramatically by varying both temperature and an external magnetic field. Consider a given singlet bond with singlet-triplet energy splitting J drawn from the distribution $P[J]$. Applying a magnetic field with Zeeman energy H has no effect on the singlet energy but splits the triplet manifold. At low temperatures $T \ll H$ this bond contributes to heat capacity only when its ground state crosses over from the singlet state to the field-polarized triplet state: the width of this resonance $|J - H| < k_B T$ (Fig. 1) is set by temperature giving a heat capacity that rises linearly in T . The distribution of bond energies enters only through the H -dependent coefficient: $C \sim T/H^\gamma$ at $T \ll H$ where $C \sim T^{1-\gamma}$ at $H = 0$. (We have set the magnetic moment to be unity.)

Given this expected scaling it came as a surprise that new experiments of Ref. 9 found a different scaling behavior on the spin-1/2 magnet $H_3LiIr_2O_6$, a member of the family of so-called Kitaev honeycomb iridates¹⁰. Both magnetic frustration and disorder are likely ingredients in this compound: exchanges between Ir^{4+} effective spin-1/2 moments may vary randomly depending on the positions of mobile hydrogen ions, and the frustration expected from iridium's strong spin-orbit coupling is evidently manifest in the lack of any ordering transition down to at least 0.05 K, less than a percent of the 100 K exchange energy scale. The bulk of the sites form a quantum paramagnetic phase, such as a spin liquid. The remaining fraction of sites was found to contribute a power-law heat capacity $C \sim T^{1/2}$ with an appropriate small coefficient as expected from a random-singlet regime; but when a magnetic field was applied, instead of T -linear heat capacity, clear *quadratic* scaling $C \sim T^2/H^{3/2}$ was observed for $T \ll H$. Furthermore, the data are found (Ref. 9 Fig. 4a) to collapse to a single scaling curve of the form $C[H, T]/T \sim H^{-\gamma} F[T/H]$ where $\gamma = 0.5$.

The work of Ref. 9 reminds us of a system we had studied earlier, $LiZn_2Mo_3O_8$. This is a layered magnet where 2/3 of the spin disappears into singlets, leaving behind 1/3 of the spins which behave almost as free spins¹²⁻¹⁴. The mechanism for this behavior is not well understood, since various theoretical proposals¹⁵⁻¹⁷ all require some form of short range tripling of the unit cell size, which has been searched for and not found¹⁴. However on symmetry grounds we again expect the prevalent non-magnetic Li/Zn site mixing disorder¹² to generate bond randomness, whose competition with singlets requires⁷ low energy spin excitations to appear. Here we focus our at-

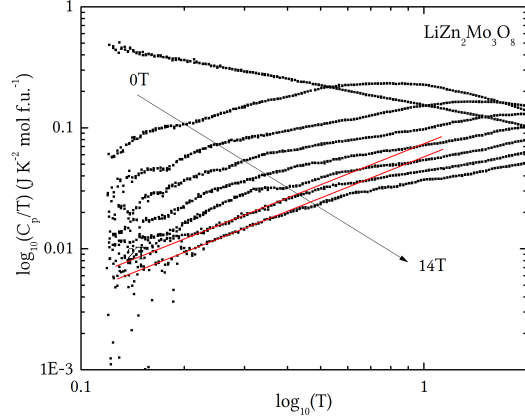


FIG. 2. **Power law heat capacity in $LiZn_2Mo_3O_8$ under various magnetic fields.** At zero field the heat capacity shows a non-integer power law $C/T \sim T^{-0.56}$, changing under various magnetic fields to functional forms with quadratic $C \sim T^2$ behavior at low temperature.

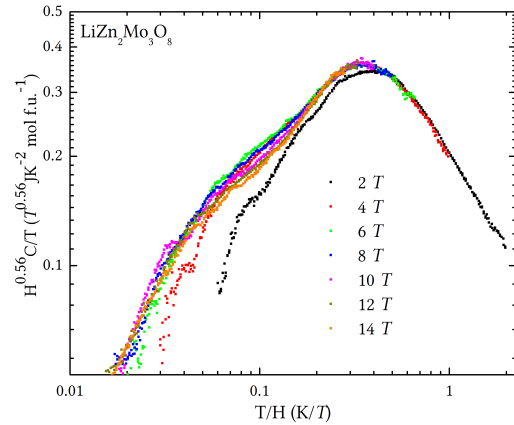


FIG. 3. **Data collapse in $LiZn_2Mo_3O_8$.** Plots from Fig. 2 rescaled by the scaling ansatz $H^{0.56}C/T$. The data collapses to a function of the single variable T/H , asymptotting as $(T/H)^2$ for $T \ll H$ and $(T/H)^{-0.56}$ for $T \gg H$, consistent with the $q = 1$ scaling theory Eq. 2 and Fig. 1.

tention on the fate of these remaining spins at low temperatures. It turns out that independent of Ref. 9, we had recognized that our previously unpublished heat capacity data (Fig. 2) also show clear data collapse with T^2 scaling (Fig. 3). Similar data collapse, though with a smaller accessible T/H window, is seen in previous heat capacity measurements¹⁸ from Ref. 11 for synthetic herbertsmithite $ZnCu_3(OH)_6Cl_2$ (Fig. 4). These materials, and related ones which we will discuss further below — 1T-TaS₂, YbMgGaO₄, YbZnGaO₄ and Ba₂YMoO₆ — differ in their spin-1/2 lattices, magnetic Hamiltonians,

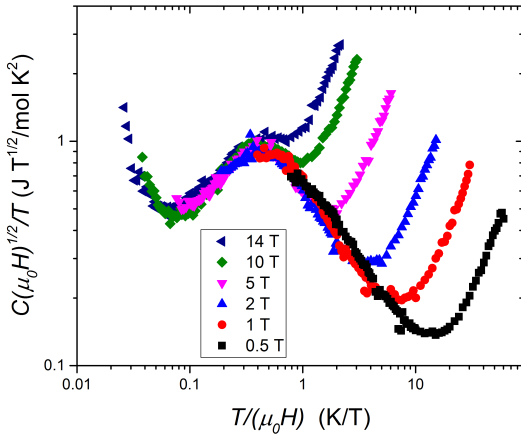


FIG. 4. **Data collapse in synthetic herbertsmithite $\text{ZnCu}_3(\text{OH})_6\text{Cl}_2$.** Data collapse for heat capacity in herbertsmithite taken from Ref. 11, here plotted with the scaling ansatz $H^{0.5}C/T$ (per formula unit of $\text{ZnCu}_3(\text{OH})_6\text{Cl}_2$). The phonon contribution has not been subtracted, which accounts for the upturn for $T/H \gtrsim 1$. Away from the upturn at low $T/H \lesssim 0.05$, which is due to the nuclear Schottky contribution, the data collapses with a peak consistent with the scaling function Eq. 2 and Fig. 1.

spatial symmetries, and sources of randomness; but their lack of magnetic order down to the lowest temperatures measured, the presence of some randomness, and the observed power-law scaling laws consistent with a contribution from a fraction of sites, taken together call for a unified theoretical framework.

In this work we argue that the missing factor of T/H needed to explain the more recent data is captured by an extension of the random-singlet theory that includes spin-orbit coupling (SOC) and its interplay with spatial symmetries, in particular through antisymmetric Dzyaloshinskii-Moriya (DM) spin exchanges. We will show how this produces three possibilities for T dependence of heat capacity in a magnetic field, associated with data collapse in T/H and a scaling exponent that can take one of three integer values.

The derivation of the T -linear scaling shown in Fig. 1 assumed that the downshifted triplet state crosses the singlet state freely. This assumption no longer holds in the presence of spin orbit coupling. The triplet will in general be split but in a magnetic field one level will still move down to approach the ground state with a modified g factor. Any off-diagonal matrix element D will mix these states, leading to level repulsion and resulting in an additional, independent, constraint $D < T$ supplementing the diagonal constraint $|J - |H|| < T$. It is important to note spin-orbit coupling is a necessary but not sufficient ingredient for the level repulsion: spin-orbit coupling modifies the magnetic exchanges in two distinct ways depending on spatial symmetries. With an inversion center at the bond midpoint, or certain other

combinations of symmetries, the matrix $J_{ij}^{\alpha\beta}$ of the spin exchange $J_{ij}^{\alpha\beta}S_i^\alpha S_j^\beta$ is required to be symmetric. The two-spin singlet state is odd under the inversion symmetry and does not mix with the triplet manifold. However without these symmetries, the spin exchange matrix gains an antisymmetric contribution to $J_{ij}^{\alpha\beta}$ which is conventionally described by the DM term $\vec{D} \cdot (\vec{S}_i \times \vec{S}_j)$. The magnitude of the DM vector \vec{D} is linear in the strength of SOC for weak SOC. By breaking inversion symmetry $i \leftrightarrow j$ it mixes the singlet and the triplet and produces the desired level repulsion.

The preceding argument may be considered in more detail. While the zero-field splitting is given simply by $(1/2)\sqrt{J^2 + |\vec{D}|^2}$, in a magnetic field this splitting becomes (Appendix 1)

$$\Delta E = \frac{1}{2\sqrt{2}}\sqrt{2(|H| - J)^2 + D_1^2 + D_2^2} \quad (1)$$

where D_1, D_2 are the components of the DM vector \vec{D} that lie perpendicular to the magnetic field \vec{H} . It is clear that each component of the DM vector \vec{D} that enters into the resonance condition Eq. 1 contributes a factor of T/D to the scaling of specific heat at low T (Appendix 3). Furthermore, as long as the ratio of DM interactions to symmetric exchange interactions remains roughly fixed in the RG flow, these factors can be replaced by T/H . We show that this is indeed the case within the strong-disorder-RG renormalization step (Appendix 2). The details of the scaling functions can depend on crystal symmetry as well as the dimensionality of the magnetic lattice (Appendix 4). We thus find three possibilities: the linear scaling $C[T] \sim T/H^\gamma$ may stay the same or gain a factor linear or quadratic in T/H .

This result can be captured by a general scaling function F_q for the density of states as measured by heat capacity,

$$\begin{aligned} \frac{C[H, T]}{T} &\sim \frac{1}{H^\gamma} F_q \left[\frac{T}{H} \right] \\ F_q[X] &\sim \begin{cases} X^\gamma & X \ll 1 \\ X^{-\gamma} (1 + \frac{c_0}{X^2}) & X \gg 1 \end{cases} \end{aligned} \quad (2)$$

The sub-dominant scaling term at large T/H must be added in order to satisfy the Maxwell relation between entropy and magnetization. A related subdominant term must be added to the scaling of magnetization at $T \ll H$ yielding $M/H \sim H^{-\gamma} (1 - m_1(T/H)^{q+2})$ (for m_1 and further discussion see Appendix 5). Here the coefficient c_0 is given by $c_0 = ((1 + \gamma)\gamma/2)/(C_{H=0}/T\chi_{H=0})$ when the zero-field susceptibility is $\chi_{H=0} \sim T^{-\gamma}$. This scaling form shows the familiar non-universal exponent $0 \lesssim \gamma \lesssim 1$ that characterizes the random-singlet distribution, but in addition a new integer index q appears that takes one of the three values $\{0, 1, 2\}$ for the three cases described above; its choice depends on the interplay of SOC with spatial symmetries as we will discuss below.

Two different values of q are necessary to capture the observed experimental scaling we are aware of so far. We have already discussed the quadratic scaling ($q = 1$) observed for $\text{H}_3\text{LiIr}_2\text{O}_6$ and $\text{LiZn}_2\text{Mo}_3\text{O}_8$. The $q = 1$ scaling in these layered magnets may be understood as arising from a DM vector that is forced to point perpendicular to the lattice plane by an approximate reflection symmetry across the plane that emerges during the course of RG flow: in each strong-disorder RG step the new spin exchanges are generated based on the pattern of valence bonds that have been integrated out at higher energies, and for a 2D lattice any such configuration of valence bonds preserves the mirror reflection across the plane, leading (Appendix 4) to a single-component DM vector and $q = 1$.

In Fig. 4 we show the data collapse for the well studied spin-1/2 kagome lattice material $\text{ZnCu}_3(\text{OH})_6\text{Cl}_2$. It is known that approximately 15% of the Zn sites which are off the kagome planes are replaced by Cu, forming $S=1/2$ local moments¹⁹. Furthermore, there is significant DM coupling. We should mention two caveats. First the nuclear contribution makes the low temperature spin contribution inaccessible and second, the bulk spin gap is estimated to be 0.7 meV, so that the high field data may have some bulk contribution due to the closing of the spin gap. With these reservations, the data collapse shown in Fig. 4 may also be consistent with the $q = 1$ case.

Next we consider the layered material 1T-TaS₂, where a charge density wave (CDW) transition at intermediate temperatures leads to a cluster Mott insulator with one spin-1/2 per 13-site unit cell arranged into a triangular lattice, with phenomenology consistent with a spin liquid state²⁰. A small fraction of the spins (less than than a few % per cluster) were recently observed to produce a low temperature T -linear term in the heat capacity with a coefficient that decreases monotonically with a magnetic field (Ref. 21 Fig. 4) roughly as $C \sim H^{-2/3}T$. This is consistent with the argument above for linear scaling ($q = 0$) for 1T-TaS₂ due to its high crystal symmetry, preserved even in the CDW state, that forbids DM interactions from being generated for not only nearest neighbor and second neighbor bonds but further neighbor bonds as well. A replot of the $C[H, T]$ two-parameter data indeed showed²² data collapse consistent with Eq. 2 with $q = 0$.

It will be interesting to test the data collapse scaling form for other frustrated spin-1/2 quantum magnets. Other layered compounds such as YbMgGaO_4 and YbZnGaO_4 , both with effective spin-1/2 moments from Yb arranged on a triangular lattice and with intrinsic Mg/Ga and Zn/Ga charge disorder^{23,24} show clear $C \sim T^{1-\gamma}$ scaling in zero field measurements^{23,25,26}; but the $T \ll H \ll J_0$ scaling limit, given the small lattice magnetic exchange energy $J_0 \sim \text{few K}$, is not yet clear. The case $q = 2$ is expected to arise most naturally in magnets with fully 3D magnetic lattices such as Ba_2YMoO_6 ²⁷, which we leave for future work.

Finally, we note that the appearance of scaling and data collapse sheds light on two interrelated subsystems of the quantum magnet. The first subsystem is formed by the local moments that contribute to the heat capacity scaling. When the material disorder does not directly change the sites of its spin-1/2 lattice but rather impacts it (weakly or strongly) only through bond randomness in the magnetic exchanges — likely the case for all the materials discussed above except synthetic herbertsmithite — then the local moment subsystem is *emergent* via an unusual RG flow⁷. The quantum critical scaling forms which can be exhibited by this subsystem are interesting both in their own right and as a signature of a coexisting quantum paramagnet state for the second subsystem, consisting of the remaining spins. This coexisting quantum paramagnetic phase must involve valence bonds which may be frozen, possibly with a relic of valence-bond-solid order, or resonating, as in a quantum spin liquid and associated topological order. The interplay of the quantum paramagnet with the local moments that produce the T/H scaling merits further exploration.

Acknowledgments. IK thanks Adam Nahum and T. Senthil for discussions and instrumental related work, and Martin Mourigal for many relevant discussions. TMM and JPS acknowledge Oleg Tchernyshyov for useful discussions. We thank Joel Helton and Young Lee for discussions and for permission to show the data collapse plot Fig. 4. We thank Hidenori Takagi for discussions. We also thank Yoram Dagan and Itai Silber for sharing their data and plots for 1T-TaS₂. IK acknowledges support by the Pappalardo fellowship at MIT. The work at IQM was supported by the U.S. Department of Energy, office of Basic Energy Sciences, Division of Materials Sciences and Engineering under Grant No. DEFG02-08ER46544. TMM acknowledges support of the David and Lucile Packard foundation. PAL acknowledges the support of DOE Grant No. DE-FG02-03-ER46076.

APPENDIX

This appendix contains details for the calculations described in the main text. It is structured as follows. We begin by considering the effect of DM interactions on modifying the two-spin singlet state, as well as the competition of these effects with an applied magnetic field. We then consider the RG flow under the basic strong disorder RG (SDRG) step, as appropriate for random singlets, in the presence of DM interactions. Then we compute the expected scaling phenomenology and discuss the various cases for q . Finally we relate the scaling forms for various observables including heat capacity, NMR lifetimes and magnetization.

1. Two spins with DM interactions

To see the effects of DM interactions on the valence bond states, consider the following Hamiltonian for two spins i, j ,

$$\mathcal{H}_{ij} = J(\vec{S}_i \cdot \vec{S}_j) + \vec{D} \cdot (\vec{S}_i \times \vec{S}_j) - \vec{H} \cdot (\vec{S}_i + \vec{S}_j) \quad (3)$$

where in addition to a general DM term and magnetic field, for simplicity here the symmetric spin interactions are taken to consist of pure Heisenberg exchange; below we discuss generic SO(3) breaking exchanges. Defining the total spin operator $\vec{S}_{\text{tot}} \equiv \vec{S}_i + \vec{S}_j$, the Hamiltonian up to an overall energy shift may be written as

$$\mathcal{H}_{ij} = \frac{J}{2}(\vec{S}_{\text{tot}})^2 + \frac{|D|}{2}(T_D + T_D^\dagger) - \vec{H} \cdot \vec{S}_{\text{tot}} \quad (4)$$

where the DM term mixes the singlet with the member of the triplet manifold that has zero total spin moment along the DM vector,

$$T_D \equiv i |\text{singlet}\rangle\langle\text{triplet}; (\vec{S}_{\text{tot}} \cdot \vec{D} = 0) | \quad (5)$$

At zero field $H = 0$, the ground state is a mixture of the spin-singlet state and this $\vec{S}_{\text{tot}} \cdot \vec{D} = 0$ member of the triplet manifold, set by the Hamiltonian matrix $2\mathcal{H}_{H=0} = J\sigma^3 + |D|\sigma^2$ acting on the basis of these two states. The ground state is nondegenerate; for small D/J , it is modified from the singlet state only perturbatively in D/J .

For larger fields near resonance $H \approx J$ it is useful to project the Hamiltonian to the low energy space spanned by the singlet and the member of the triplet with maximal total magnetization along the magnetic field direction. In this 2-level subspace, the Hamiltonian, again up to a constant, is

$$\mathcal{H}_{H \approx J} = \frac{1}{2}(|H| - J)\sigma^3 + \frac{1}{2\sqrt{2}}(D_1\sigma^2 - D_2\sigma^1) \quad (6)$$

where σ are Pauli matrices acting on the (singlet, total-spin-up-triplet) basis, and D_1, D_2 are the components of the DM vector perpendicular to the magnetic field axis.

Indeed this equation, with modified parameters, describes the general scenario reached by adding generic spin-orbit-coupled interactions to the symmetric spin exchange matrix $J_{ij}^{\mu\nu} S_i^\mu S_j^\nu$. Without the DM term the singlet state remains an eigenstate and we shall assume the symmetric exchanges are sufficiently antiferromagnetic so that the singlet is the ground state of $J_{ij}^{\mu\nu} S_i^\mu S_j^\nu$. The triplet-manifold eigenstate brought down by the field is modified. The resulting Hamiltonian is described by Eq. 6 with J interpreted as an effective exchange parameter that may depend on the direction of \vec{H} , and D_1, D_2 interpreted as two particular components of the DM vector.

2. Strong-disorder RG step: integrating out two spins with DM interactions

The strong disorder RG (SDRG) step entails integrating out a pair of spins and considering the renormalization of interaction for every other remaining pair. It thus suffices to look at each cluster of four spins containing the strong pair. We assume weak DM interactions; this is the case for weak spin-orbit coupling as well as for strong spin-orbit coupling with some approximate microscopic or emergent inversion or mirror symmetries. As the starting point for an SDRG step we must postulate that the quantum state of a portion of the system, namely the fraction of spins that participate in the random-singlet-type regime, is described by a power law distribution of exchange energies. Computing the SDRG step in the presence of weak DM interactions, we find that in 1D the DM and Heisenberg terms scale identically, while in 2D they scale at the same order with some distinctions in detail. The resulting “random-singlet” state has each spin paired with another into a nondegenerate frozen state, that differs from the spin-singlet state by the addition of a spin quadrupole (nematic) moment that preserves time-reversal, as is anyway required by the lack of spin rotation symmetry.

Consider a pair (1,2) of strongly coupled spins, with Heisenberg exchange J_{12} as well as DM exchange D_{12} , and consider weak Heisenberg interactions between spins 1,2 and two additional spins 3,4. The ground state of $H_{12} = J_{12}H_{12}^{\text{Heis}} + D_{12}H_{12}^{\text{DM}}$ is no longer a spin-singlet under spin rotations, but nevertheless is a unique state. The low energy manifold has spins 1,2 in the ground state of H_{12} , while the bare interactions H_{34}^0 gain a renormalized contribution by virtual excitations of the (1,2) excited states, as $H_{34}^0 \rightarrow H_{34}^0 + \Delta H_{34}$. We compute ΔH_{34} within second order perturbation theory in $1/J_{12}$. We find $\Delta H_{34} = J_{34}H_{34}^{\text{Heis}} + D_{34}H_{34}^{\text{DM}}$ with renormalized Heisenberg and DM interactions set by

$$J_{34} = \frac{(J_{14} - J_{24})(J_{23} - J_{13})}{2J_{12}} \quad (7)$$

$$D_{34} = \frac{D_{12}}{J_{12}} \frac{(J_{14}J_{23} - J_{13}J_{24})}{2J_{12}} \quad (8)$$

SDRG is analytically controlled in 1D. In this setting, each of the spins 1,2 interacts more strongly with a different spin 3,4; for instance, if the sites are arranged sequentially as [4,1,2,3], then one can take $J_{13} = J_{24} = 0$. Then the sign of the (antiferromagnetic) Heisenberg exchange is preserved under the SDRG. Moreover, here we see that in this controlled setting, the Heisenberg and DM interactions renormalize identically, preserving their ratio $|D_{34}|/J_{34} = |D_{12}|/J_{12}$. (Recall that the sign of the DM term depends on the convention of orientation of the bond.) In general, we see that the Heisenberg and DM terms scale qualitatively similarly, so one expects that a weak bare DM term will remain a spectator to the standard picture of SDRG.

3. Derivation of scaling in a magnetic field

The entropy distribution at low energies is set by the distribution of Hamiltonian parameters. Consider the distribution of bonds picked by the strong-disorder RG. This defines the (highly correlated) distributions of three energy parameters: (1) the symmetric splitting J ; (2) the antisymmetric splitting set by the components D_i of the DM vector \vec{D} ; (3) the resulting true splitting between the lowest state and the second state. Let us denote the distributions of these parameters by P_1, P_2, P_3 respectively. The Hamiltonian matrix elements for the lowest two states are given above, and the resulting splittings are as follows. With no magnetic field, this splitting is

$$\Delta E[H = 0] = \frac{1}{2} \sqrt{J^2 + |D|^2} \quad (9)$$

In a magnetic field, this splitting (see Eq. 6) becomes

$$\Delta E = \frac{1}{2\sqrt{2}} \sqrt{2(|H| - J)^2 + D_1^2 + D_2^2} \quad (10)$$

where D_1, D_2 are the components of the DM vector that lie perpendicular to the magnetic field \vec{H} . The entropy distribution seen directly by $C[T]$ at zero field is the distribution of the splittings $P_3[E]$. Self consistency within the strong-disorder RG framework requires a broad tail for $P_3[E]$, generally power law $P_3[E] = E^{-\gamma}$, with γ defined by the specific heat exponent at zero field,

$$C[H = 0][T] \sim T^{1-\gamma}.$$

Now let us add a magnetic field and consider the scaling of specific heat at temperatures far below the Zeeman energy, $T \ll H$.

First recall the case of no DM interactions, $D = 0$. Here the field picks out the distribution $P_3[H]$, ie P_3 at energy $\Delta E = H$. Now we may linearize P_3 for energy splittings E near $\Delta E = H$. It has an analytic polynomial expansion, which to first order may be written as $P_3[E] = P_3[H] + c_1(E - H)$. The specific heat picks out all states with energy $\Delta E < T$. Due to the linearization, $C[H, T] \approx T P_3[H]$.

Now consider the case of small but nonzero DM interactions. Let us count the states with excitation energy $\Delta E < T$. J is set by the distribution $P_1[J - H] = P_1[H] + c_1(J - H)$. The conditional distribution for each component D_i of the DM vector \vec{D} , conditioned on being given a bond with a particular Heisenberg exchange $J \approx H$, may be taken to be approximately Gaussian with some width set by this $J \approx H$. To reach a resonance with $\Delta E < T$ in the regime where $T \ll H$, we must have $D_i \ll H$ and thus the distribution of D_i of interest here is uniform and may be approximated by its value at the origin, $P_2[D_i] \approx P_2[0]$. Since the width of the distribution P_2 is proportional to $J \approx H$, normalization sets its overall amplitude by a factor proportional to $1/J \approx 1/H$, giving $P_2[D_i] \approx P_2[0] = c_2/H$. The number of states with $\Delta E < T$ is then given by $T P_1[H] \sim T/H^\gamma$ times a factor of T/H for each relevant component D_i .

4. Scaling of specific heat in a magnetic field

Due to quantum mechanical level repulsion, a low excitation energy $\Delta E < T$ entails conditions on the amplitude of three parameters: $||H| - J| < T$, $|D_1| < T$, and $|D_2| < T$. We must now consider three distinct physical scenarios, depending on the crystal symmetries or the effective approximate symmetries that emerge in SDRG, as well as potentially depending on the direction of the magnetic field. Recall that the scaling relation is $C[H, T] \sim T^{1-\gamma}$ for $H \ll T$, and is

$$C[H, T] \sim \frac{T^{q+1}}{H^{q+\gamma}} \quad (11)$$

for $T \ll H$.

Case (1): $\vec{D} \times \vec{H} = 0$. This is the case if symmetries constrain the DM vector to lie along a particular axis, and the magnetic field is taken to lie along the same axis. Then the specific heat scaling reduces to the case with no DM terms, and we find $q = 0$.

Case (2): only one component of \vec{D} perpendicular to \vec{H} is nonzero. This is the case if symmetries constrain the DM vector to lie along a particular axis, for any magnetic field direction away from that special axis (or for a powder average).²⁸ For example, this can occur when there is a mirror symmetry consisting of reflection across the 2D plane: this symmetry constrains \vec{D} to lie perpendicular to the plane. Even if the crystal does not have such a symmetry microscopically, it may be reasonable to expect that, within a 2D magnetic layer, the magnetic exchanges that develop under RG will depend only on the single layer, and that such a mirror symmetry may emerge as an approximate symmetry under RG. In particular, within an approximation where each magnetic layer is treated independently as a purely 2D system, a given SDRG step will involve only the configuration of valence bonds within the 2D layer that was generated in previous RG steps, and reflection across the plane becomes a symmetry. In this case, only one component D_i is relevant, and we find $q = 1$.

Case (3): both D_1, D_2 are nonzero. This is the case if no symmetries constrain the DM vector. (This is also the case if symmetries constrain the DM vector to lie in a plane, and the magnetic field is oriented perpendicular to this plane.) Then both D_1, D_2 are relevant, and we find $q = 2$.

Thus we find a different scaling form, with different powers of T/H , depending on the crystal or emergent symmetries as well as the direction of the magnetic field. The linear scaling of 1T-TaS₂ ($q = 0$) may be understood by noting that the inversion centers in the 1T-TaS₂ crystal structure forbid DM interactions from being generated not only for nearest-neighbor bonds but also for 2nd, 3rd, 4th, etc neighbors, so it may be reasonable that no sizable DM interactions arise during RG. Quadratic scaling ($q = 1$), as in H₃LiIr₂O₆ and LiZn₂Mo₃O₈, can arise for generic or powder-averaged field directions through

an emergent approximate mirror symmetry consisting of reflections across the 2D layer, a reasonable scenario for layered magnets. Cubic scaling ($q = 2$) may thus be expected to arise in valence bond materials with 3D lattices, such as Ba_2YMoO_6 ²⁷. Experimental observation of the $q = 2$ case is left for future work.

5. Magnetization scaling and NMR $1/T_1$

It is instructive to contrast the heat capacity with other experimental quantities. Magnetization, in particular, does not access the same information on the entropy of the spectrum. Magnetization and susceptibility scaling has been previously discussed for SO(3) random singlets in the context of doped semiconductors^{29–31}, as well as theoretically³² in the context of observed susceptibility scaling from the dilute impurity spins of synthetic herbertsmithite³³; the scaling is $M[H, T] \sim H^{1-\gamma}$ for $T \ll H$ and $M[H, T] \sim HT^{-\gamma}$ for $H \ll T$.³⁴ Note that magnetization at $T \ll H$ is determined by counting all states with $J < H$: any information on the low energy states with $\Delta E < T$, which determine the specific heat scaling $C[H, T]$, is not captured by the magnetization or susceptibility at $T \ll H$. In particular the presence of weak DM interactions does not modify these expressions for magnetization or susceptibility scaling.

Interestingly however, Maxwell's relation between entropy and magnetization gives an additional subdominant correction to the magnetization scaling at $T \ll H$; this correction encapsulates the heat capacity and does involve the q exponent. Observe that the Maxwell relation $\partial S/\partial H = \partial M/\partial T$ (required by a thermodynamic potential $G[H, T]$ with $\text{curl}[\text{grad}[G[H, T]]] = 0$) conveys information about the entropy to the temperature derivative of magnetization. At $T \ll H$ the conventional magnetization scaling is expressed as $M \sim H^{1-\gamma}$ giving $\partial M/\partial T = 0$. Maxwell's relation is satisfied by adding a subdominant negative term to the $T \ll H$ magnetization scaling, yielding the scaling function

$$\begin{aligned} \frac{M[H, T]}{H} &\sim \frac{1}{H^\gamma} F_q^M \left[\frac{T}{H} \right] & (12) \\ F_q^M[X] &\sim \begin{cases} 1 - m_1 X^{q+2} & X \ll 1 \\ X^{-\gamma} & X \gg 1 \end{cases} \end{aligned}$$

Since we are in the $T \ll H$ regime, this additional $(T/H)^{q+2}$ correction is quite small. This subdominant magnetization scaling coefficient is given by $m_1 = (q + \gamma)/((q + 1)(q + 2))((C/M)(H/T)^{q+1})[T=0]$ when heat capacity $C \sim H^{-q-\gamma}T^{q+1}$. This relation between the entropy measured in $C[H, T]$ and the magnetization $M[H, T]$ is also visible in the experimental data of Ref. 9. There magnetization was found to obey a scaling relation that appears to be roughly captured by $M \sim HT^{-1/2}$ for $H \ll T$, and, for $T \ll H$, $M \sim H^{1/2}$ with an additional subdominant correction consistent with a $(T/H)^3$ term added with a negative sign. Taking $\gamma \approx 1/2$ as extracted independently from the scaling of specific heat at zero field, these measurements are consistent with the theoretical expectations.

The scaling of heat capacity, equivalent to the scaling of the entropy, is also closely related to the scaling of $1/T_1 T$ where T_1 is the NMR spin-lattice relaxation time. The quantity $(T_1 T)^{-1}$ is related to the momentum-averaged (local) imaginary part of the spin susceptibility. Thus it serves as a measure of the spin-carrying states in the spectrum. NMR $1/T_1$ measurements complement the heat capacity by providing the information that the gapless spectrum carries spin excitations — nontrivial information for weak SOC, which is of course satisfied by the spectrum associated with breaking valence bonds.

Note however that the broad distribution of couplings inherently implies that the spin-lattice relaxation, measured by the NMR lifetime T_1 , should be described by a highly stretched exponential. A fit to an exponential with a single lifetime T_1 will likely not be appropriate. (When considering a single lifetime T_1 , it is worth noting that the NMR Korringa law is a fine tuned case appropriate only for a metal: more generally the $1/T_1$ is linear in the density of states, $1/T_1 \sim C/\Gamma$ with some lifetime Γ which is a priori not related to the density of states, and not known.) In general there may be two contributions to the spin-lattice relaxation: one from the minority of spins that participate in the random-singlet scaling, and another from the phase of the bulk of the sites. However generally the fluctuations will be dominated by the few sites in the tail of the energy distribution, i.e. the minority of spins in the random-singlet regime, producing a continuum of lifetimes for the spin-lattice relaxation and rendering exponential decay fits with a single lifetime T_1 difficult to interpret.

¹ L. Balents, *Nature* **464**, 199 (2010).

² C. Dasgupta and S.-k. Ma, *Phys. Rev. B* **22**, 1305 (1980).

³ D. S. Fisher, *Phys. Rev. B* **50**, 3799 (1994).

⁴ R. N. Bhatt and P. A. Lee, *Journal of Applied Physics* **52**, 1703 (1981), <http://aip.scitation.org/doi/pdf/10.1063/1.329684>.

⁵ R. N. Bhatt and P. A. Lee, *Phys. Rev. Lett.* **48**, 344 (1982).

⁶ M. A. Paalanen, J. E. Graebner, R. N. Bhatt, and S. Sachdev, *Phys. Rev. Lett.* **61**, 597 (1988).

⁷ I. Kimchi, A. Nahum, and T. Senthil, ArXiv e-prints (2017), arXiv:1710.06860 [cond-mat.str-el].

⁸ As may be required by the conjectured disordered-Lieb-Schultz-Mattis restrictions⁷.

⁹ K. Kitagawa, T. Takayama, Y. Matsumoto, A. Kato, R. Takano, Y. Kishimoto, S. Bette, R. Dinnebier, G. Jackeli, and H. Takagi, *Nature* **554**, 341 (2018), <http://rdcu.be/GYFa>.

¹⁰ M. Hermanns, I. Kimchi, and J. Knolle, ArXiv e-prints

¹¹ (2017), arXiv:1705.01740 [cond-mat.str-el].

¹² J. S. Helton, K. Matan, M. P. Shores, E. A. Nytko, B. M. Bartlett, Y. Yoshida, Y. Takano, A. Suslov, Y. Qiu, J.-H. Chung, D. G. Nocera, and Y. S. Lee, *Phys. Rev. Lett.* **98**, 107204 (2007).

¹³ J. P. Scheckelton, J. R. Neilson, D. G. Soltan, and T. M. McQueen, *Nature Materials* **11**, 493 (2012).

¹⁴ J. P. Scheckelton, F. R. Foronda, L. Pan, C. Moir, R. D. McDonald, T. Lancaster, P. J. Baker, N. P. Armitage, T. Imai, S. J. Blundell, and T. M. McQueen, *Phys. Rev. B* **89**, 064407 (2014).

¹⁵ M. Mourigal, W. T. Fuhrman, J. P. Scheckelton, A. Wartelle, J. A. Rodriguez-Rivera, D. L. Abernathy, T. M. McQueen, and C. L. Broholm, *Phys. Rev. Lett.* **112**, 027202 (2014).

¹⁶ R. Flint and P. A. Lee, *Phys. Rev. Lett.* **111**, 217201 (2013).

¹⁷ G. Chen, H.-Y. Kee, and Y. B. Kim, *Phys. Rev. B* **93**, 245134 (2016).

¹⁸ G. Chen and P. A. Lee, *Phys. Rev. B* **97**, 035124 (2018).

¹⁹ We thank Joel Helton and Young Lee for permission to show this data collapse plot Fig. 4.

²⁰ T.-H. Han, M. R. Norman, J.-J. Wen, J. A. Rodriguez-Rivera, J. S. Helton, C. Broholm, and Y. S. Lee, *Phys. Rev. B* **94**, 060409 (2016).

²¹ K. T. Law and P. A. Lee, *Proceedings of the National Academy of Sciences* **114**, 6996 (2017), <http://www.pnas.org/content/114/27/6996.full.pdf>.

²² A. Ribak, I. Silber, C. Baines, K. Chashka, Z. Salman, Y. Dagan, and A. Kanigel, *Phys. Rev. B* **96**, 195131 (2017).

²³ Y. Li, H. Liao, Z. Zhang, S. Li, F. Jin, L. Ling, L. Zhang, Y. Zou, L. Pi, Z. Yang, J. Wang, Z. Wu, and Q. Zhang, *Scientific Reports* **5**, 16419 (2015).

²⁴ Y. Li, D. Adroja, D. Voneshen, R. I. Bewley, Q. Zhang, A. A. Tsirlin, and P. Gegenwart, *Nat. Comm* **8**, 15814 (2017).

²⁵ Y. Xu, J. Zhang, Y. S. Li, Y. J. Yu, X. C. Hong, Q. M. Zhang, and S. Y. Li, *Phys. Rev. Lett.* **117**, 267202 (2016).

²⁶ Z. Ma, J. Wang, Z.-Y. Dong, J. Zhang, S. Li, S.-H. Zheng, Y. Yu, W. Wang, L. Che, K. Ran, S. Bao, Z. Cai, P. Čermák, A. Schneidewind, S. Yano, J. S. Gardner, X. Lu, S.-L. Yu, J.-M. Liu, S. Li, J.-X. Li, and J. Wen, *Phys. Rev. Lett.* **120**, 087201 (2018).

²⁷ M. A. de Vries, A. C. McLaughlin, and J.-W. G. Bos, *Phys. Rev. Lett.* **104**, 177202 (2010).

²⁸ Case (2) can also occur if symmetries constrain the DM vector to lie in a plane and the magnetic field is not oriented perpendicular to this plane.

²⁹ R. N. Bhatt, *Physica Scripta* **1986**, 7 (1986).

³⁰ M. P. Sarachik, A. Roy, M. Turner, M. Levy, D. He, L. L. Isaacs, and R. N. Bhatt, *Phys. Rev. B* **34**, 387 (1986).

³¹ A. Roy, M. Sarachik, and R. Bhatt, *Solid State Communications* **60**, 513 (1986).

³² R. R. P. Singh, *Phys. Rev. Lett.* **104**, 177203 (2010).

³³ J. S. Helton, K. Matan, M. P. Shores, E. A. Nytko, B. M. Bartlett, Y. Qiu, D. G. Nocera, and Y. S. Lee, *Phys. Rev. Lett.* **104**, 147201 (2010).

³⁴ Large spin clusters which may arise in the course of the RG flow can contribute additional Curie (free spin) terms to the magnetization and susceptibility scaling.